Differential effect of sunitinib on the distribution of temozolomide in an orthotopic glioma model

Qingyu Zhou and James M. Gallo

Department of Pharmaceutical Sciences, School of Pharmacy, Temple University, Philadelphia, PA, USA

Normalization of tumor vasculature by antiangiogenic agents may improve the delivery of cytotoxic drugs to the tumor, leading to more effective therapy. In this study, we used pharmacokinetic and pharmacodynamic approaches to investigate how sunitinib at different dose levels affects brain distribution of temozolomide (TMZ), and to ascertain the relationship between intratumoral TMZ concentrations and tumor vascularity in an orthotopic human glioma model. Three groups of intracerebral U87MG tumor-bearing mice were given either vehicle or sunitinib at 20 mg/kg or 60 mg/kg per day for 7 days before receiving a steady-state regimen of TMZ that consisted of an intravenous bolus and a 3-h intraarterial infusion. TMZ concentrations in plasma, normal brain, and brain tumor were determined, and several biomarkers related to the antiangiogenic activity of sunitinib were examined. TMZ distribution in the normal brain as indicated by the brain-to-plasma steady-state TMZ concentration ratios was analogous across the three treatment groups. The brain tumor-to-plasma steady-state TMZ concentration (ss C_t/C_p) ratio was significantly increased in the 20 mg/kg sunitinib group (0.98 ± 0.17) compared with the control (0.76 ± 0.17) and 60 mg/kg sunitinib (0.68 ± 0.09) groups. The ss C_t/C_p ratios were significantly correlated with the vascular normalization index (VNI), derived from the expression of CD31, collagen IV, and α-smooth muscle actin, which represents the fraction of functioning vessels out of the total tumor vessels. In conclusion, the effect of sunitinib on the brain tumor distribution of TMZ was dose dependent and indicated that optimal tumor exposure was achieved at a lower dose and was associated with the VNI. *Neuro-Oncology 11, 301–310, 2009 (Posted to Neuro-Oncology [serial online], Doc. D08-00131, October 29, 2008. URL http://neuro-oncology.dukejournals.org; DOI: 10.1215/15228517-2008-088)*

Keywords: antiangiogenic therapy, combination chemotherapy, pharmacokinetics, sunitinib, temozolomide, vascular normalization

Glioblastoma multiforme is the most common and lethal type of primary brain tumor with a median survival duration of only 12 months[1] and a 3-year survival rate of less than 2%.[2] Despite recent advances in neuroimaging, surgery, radiotherapy, and chemotherapy as well as remarkable progress in characterizing the molecular pathogenesis of gliomas,[3] these tumors remain incurable and have eluded effective therapeutic intervention, partly due to their inherent molecular heterogeneity. New therapeutic agents are desperately needed to improve survival rates and to eventually cure patients of this deadly disease. Malignant gliomas are highly vascularized, and increasing vascularity has been correlated with increasing grade.[4,5] In this regard, therapeutic strategies that target tumor vasculature are particularly appealing because endothelial cells in the tumor microenvironment that compose blood vessels are thought to be genetically stable and unlikely to develop drug resistance.

Tumors are believed to activate the angiogenic switch by increasing the production of endogenous angiogenesis stimulators and/or decreasing the secretion of angiogenesis suppressors.[6,7] A variety of antiangiogenic agents are under development that target molecular pathways

Received May 20, 2008; accepted October 10, 2008.

Address correspondence to James M. Gallo, Department of Pharmaceutical Sciences, School of Pharmacy, Temple University, 3307 North Broad St., Philadelphia, PA 19140, USA (jmgallo@temple.edu).

Copyright 2009 by the Society for Neuro-Oncology

involved in cell signaling during new vessel formation.[8,9] The prevailing evidence indicates that more than one angiogenic signaling network is capable of driving tumor angiogenesis,[10] and thus, it is conceivable that a compound that blocks multiple target sites may be more potent in inhibiting angiogenesis than one that targets a single cell-surface receptor. One such broad-spectrum receptor tyrosine kinase inhibitor is sunitinib. Sunitinib is an orally active indolinone-based multitargeted kinase inhibitor that inhibits several related tyrosine kinase receptors, including vascular endothelial growth factor receptors 1–3 (VEGFR1–3), platelet-derived growth factor receptors α and β, stem cell factor receptor, FMS-like tyrosine kinase 3, colony-stimulating factor receptor type 1 receptor, and the glial cell line–derived neurotrophic factor receptor.[11,12] Sunitinib has demonstrated a high level of antitumor efficacy in a range of histologically diverse xenograft models and was recently approved by the U.S. Food and Drug Administration for use in patients with advanced renal cell carcinomas and imatinib-resistant or -intolerant gastrointestinal stromal tumors.[12–17]

The potential significance of sunitinib in glioma therapy has not been fully explored despite its antitumor activity against a broad range of cancers. Previously published preclinical studies have shown that monotherapy with sunitinib was efficacious in suppressing tumor growth in subcutaneous and intracerebral glioma models,[12,16] but not in reducing brain tumor invasion.[16] No clinical studies of sunitinib for the treatment of glioblastomas have yet been published, although there were several case reports showing controversial results of sunitinib treatment in patients with brain metastases from renal cell carcinomas.[18–20] Tumors developed in highly vascularized organs, such as brain,[21,22] lung,[22,23] and liver,[24] can grow through preexistent blood vessels, a process termed "vessel co-option." Emerging evidence has suggested that brain tumors may adapt to antiangiogenic therapies by co-opting preexisting blood vessels of the brain and consequently adopt a more infiltrative growth pattern.[25–27] Rubenstein and coworkers[25] reported that treatment with an anti-VEGF antibody in an orthotopic rat glioma model resulted in the formation of satellite lesions around the primary tumors that appeared to track along existing blood vessels, which is consistent with vessel. Given the paucity of data on the effects of sunitinib in brain tumors and considering that brain tumors may infiltrate normal brain by co-option in response to sunitinib treatment, combining sunitinib with cytotoxic anticancer drugs that are able to cross the blood-brain barrier (BBB) is a logical strategy that needs to be examined in greater detail.

A growing body of evidence indicates that antiangiogenic agents can improve exposure of tumor cells to cytotoxic drugs by normalizing the aberrant vascular supply in tumors and reducing tumor interstitial fluid pressure.[28–30] In our recent study in the subcutaneous SF188 human glioma xenograft model overexpressing VEGF, we showed that once-daily oral dosing of either 10 mg/kg or 40 mg/kg sunitinib for 14 days increased temozolomide (TMZ) tumor distribution; however, only the 10 mg/kg group reached statistical significance compared with the vehicle control group. We also identified several important factors relevant to the antiangiogenic agent–induced tumor vascular normalization and proposed a vascular normalization index (VNI) that might serve to correlate the angiogenic phenotype to the distribution of cytotoxic drugs in solid tumors.[30] Although subcutaneous xenograft models allow for easy access to tumors for experimental manipulation, they neither recapitulate the complex relationship between tumor cells and the stromal microenvironment unique to each tissue,[31] nor possess the BBB that is a variable in drug penetration. Thus, in contrast to subcutaneous tumor models, orthotopic models of gliomas, which feature glioma cells growing in their natural location and possess a BBB, may more accurately reflect tumor–host and drug transport interactions, thereby replicating human gliomas with high fidelity.[32] In the present study, we sought to determine if sunitinib treatment would affect tumor exposure of TMZ in an orthotopic human glioma model. The close agreement between our previous and present studies on the dose-dependent effect of sunitinib on TMZ distribution in tumors offers a rational explanation for both compromised and enhanced therapeutic activity for this combination, which has implications for the design of clinical studies in brain tumor patients.

Materials and Methods

Materials

TMZ was generously provided by Schering-Plough Research Institute (Kenilworth, NJ, USA). Sunitinib was supplied by M.V. Reddy (Fels Institute for Cancer Research, Temple University, Philadelphia, PA, USA) and dissolved in 0.1 M citrate buffer (pH 4.7) at a stock concentration of 3 mg/ml. All other chemicals, solvents, and reagents were obtained from commercial sources.

Male NIH Swiss nude mice (nu/nu, 8–10 weeks old) were purchased from Taconic Farms (Germantown, NY, USA). All animal experiments were approved by Temple University's Institutional Animal Care and Use Committee and performed according to the guidelines of the National Institutes of Health.

U87MG human glioma cells were purchased from the American Type Culture Collection, cultured in Dulbecco's modified Eagle's medium supplemented with 10% standard fetal bovine serum, 100 U/ml penicillin, and 100 μg/ml streptomycin, and maintained in a humidified atmosphere of 5% CO_2 in air at 37°C.

Orthotopic Tumor Inoculation

Nude mice were anesthetized by an intraperitoneal dose (0.1 ml/20 g body weight) of a 3:2:1 (vol/vol/vol) mixture of ketamine hydrochloride (20 mg/ml), acepromazine maleate (2 mg/ml), and xylazine hydrochloride (4 mg/ml) and secured in a stereotactic apparatus. For tumor implantation, U87MG cells prepared fresh from culture (10^6 cells in 10 μl phosphate-buffered saline [PBS]) were

injected into the caudate putamen at a position 0.7 mm anterior and 2.2 mm lateral from the bregma and to a depth of 2.5 mm using a 10-μl Hamilton syringe (Hamilton Co., Reno, NV, USA). The animals recovered from anesthesia, were returned to the animal care facilities, and resumed their normal activity in cages.

Treatment Schedule and Pharmacokinetic Study

Twenty-four days after tumor cell implantation, tumor-bearing nude mice were randomized into three groups: (1) the vehicle control group (daily oral administration of 0.1 M citrate buffer [pH 4.7]), (2) the 20 mg/kg sunitinib group (20 mg/kg sunitinib daily p.o. for 7 days), and (3) the 60 mg/kg sunitinib group (60 mg/kg sunitinib daily p.o. for 7 days). The day after the last dose of sunitinib or vehicle, TMZ (dissolved in 0.9% NaCl containing 25% dimethyl sulfoxide) was given intravascularly to achieve steady-state plasma concentration (ss C_p) of approximately 17 μg/ml for 3 h by tail veil injection of 7.6 mg/kg of TMZ followed by a 180-min intraarterial infusion of TMZ at a rate of 133.3 μg/kg/min. At the end of the infusion, before being sacrificed, mice were anesthetized and blood samples were taken from the vena cava. Plasma was prepared by centrifugation of the heparinized blood and then stored at −80°C. After the animals were sacrificed, normal brain tissues and brain tumors were excised and halved. All tissue specimens were immediately snap-frozen on dry ice and stored at −80°C. TMZ concentrations, determined in plasma, normal brain, and brain tumor homogenate using a validated reversed-phase high-performance liquid chromatographic method with ultraviolet detection,[33] represent the steady-state concentrations of TMZ. The normal brain-to-plasma or brain tumor-to-plasma steady-state TMZ concentration ratios were calculated as an indication of TMZ's distribution in the corresponding tissue.

Immunostaining

For individual tumor samples, half the tumor was used for drug analysis and the other half for histological analysis. Cryosections (10 μm) from frozen tumors were allowed to dry in air for 30 min before being fixed in cold acetone (5 min), 1:1 acetone/chloroform (5 min), and acetone (5 min). The sections were washed with PBS and incubated with the appropriate dilutions of anti-CD31 (1:400, rat monoclonal; BD Pharmingen, San Jose, CA, USA), anti-collagen IV (1:100, rabbit polyclonal; Millipore Chemicon, Temecula, CA, USA), anti–α-smooth muscle actin (anti–α-SMA; 1:100, rabbit polyclonal; Abcam, Cambridge, MA, USA), or anti–Ki-67 (1:100, rabbit polyclonal; Abcam) primary antibodies overnight at 4°C. Subsequently, sections were rinsed with PBS and further incubated for 60 min with biotinylated antirat (for CD31) or antirabbit (for collagen IV, α-SMA, and Ki-67) immunoglobulin G (1:200; Vector Laboratories, Burlingame, CA, USA). The remaining steps were done using the Vectastain Elite ABC Kit (Vector Laboratories) for CD31 and α-SMA, or the Vectastain Alkaline Phosphatase Kit for collagen IV and Ki-67, according to the manufacturer's protocols. All sections were counterstained with 0.5% methyl green and observed by light microscope.

Terminal Deoxynucleotidyl Transferase–Mediated 2'-Deoxyuridine 5'-Triphosphate Nick-End Labeling Assay

Following preparation of 10-μm cryosections from tumors, apoptosis was quantified using a commercially available terminal deoxynucleotidyl transferase-mediated 2'-deoxyuridine 5'-triphosphate nick-end labeling (TUNEL) kit in accordance with the manufacturer's protocol (Chemicon International, Temecula, CA, USA). Briefly, cryosections (10 μm) from tumors were allowed to dry in air for 30 min before being fixed in 4% paraformaldehyde solution for 15 min. Sections were treated with a graded series of alcohol (100%, 95%, and 70% ethanol [vol/vol] in deionized water) and rehydrated in PBS (pH 7.5). Tissues were then treated with 20 ng/ml proteinase K solution for permeabilization. Endogenous peroxidase activity was quenched with 3% hydrogen peroxide in methanol. Slides were then treated with the terminal deoxynucleotidyl transferase enzyme for 1 h at 37°C, soaking in the equilibration buffer provided in the kit. Reaction was terminated by immersing the slides in the stop buffer for 15 min at room temperature. Anti-digoxigenin conjugate was added for 30 min at room temperature. After washing with PBS, slides were treated with 3,3'-diaminobenzidine solution until a light brown background appeared and then rinsed several times in deionized water. Sections were counterstained in 0.5% methyl green and observed by light microscope.

Analysis of Tumor Microvessels, Collagen IV, and α-SMA Densities, and Ki-67 Proliferation and Apoptotic Indices

Digital images (Leica DC500 camera and DM4000B microscope) were semiquantitated for CD31, collagen IV, and α-SMA in each tumor sample using Image-Pro Plus 5.1 software (Media Cybernetics, Silver Spring, MD, USA) to permit the calculation of the VNI as VNI = MVD × ($\text{density}_{\alpha\text{-SMA}}/\text{density}_{\text{collagen IV}}$), where MVD is the microvessel density determined by CD31 immunostaining and expressed as the percent CD31-positive area relative to the area of optical field; and $\text{density}_{\alpha\text{-SMA}}$ is the percent α-SMA–positive area and $\text{density}_{\text{collagenIV}}$ the percent collagen IV–positive area, relative to the area of the optical field.[30] The number of Ki-67–positive or TUNEL-positive cells was counted in five random high-power (×200) fields. The Ki-67 proliferation and apoptotic indices were calculated as the number of positive cells per total number of counted cells, expressed as a percentage. Areas with extensive necrosis were avoided.

Statistical Analysis

NCSS 2004 (Number Cruncher Statistical Systems, Keysville, UT, USA) was used for statistical evaluation

of data. All data are presented as the mean ± SD. TMZ distribution in the tumor was compared with that in the normal brain using the paired-sample *t*-test. Comparison of means among three study groups was made using one-way analysis of variance followed by the post hoc Tukey-Kramer multiple-comparison test. The Pearson correlation test was used to investigate the correlation between two variables. A two-sided *p*-value of less than 0.05 was considered statistically significant.

Results

Comparisons of TMZ Distribution in Normal Brain and Brain Tumor between Vehicle Control and Sunitinib-Treated Animals

The pharmacokinetic (PK) study was designed to evaluate the effect of sunitinib on the penetration of TMZ into brain and brain tumor under steady-state conditions, which would serve as an accurate indicator of drug distribution. The steady-state regimen employed a simultaneous intravenous bolus and continuous intraarterial infusion for 3 h, which achieved steady-state expeditiously and avoided the need for a protracted multiple-dose regimen lasting several days. Using the combined TMZ regimen of 7.6 mg/kg by intravenous bolus and a 133.3 μg/kg/min continuous intraarterial infusion, nude mice reached apparent steady-state conditions within 1.5 h. A pilot study using the same TMZ dosing regimen revealed that mean TMZ plasma concentrations were essentially constant between 1.5 and 3 h and ranged from 14.9 to 20.4 μg/ml. As shown in Table 1, the mean ss C_p values were similar in the three study groups, ranging from 16.5 to 18.6 μg/ml. Likewise, no significant differences in the mean steady-state TMZ concentrations in normal brain (ss C_b) were observed between the control and two sunitinib treatment groups (Table 1). Because microvessels supplying brain tumors only partially retain characteristics of the BBB present in normal brain,[34] we anticipated that TMZ penetration into brain tumor would be greater than that into normal brain. In line with these expectations, the mean steady-state tumor concentration (ss C_t) values in the control, sunitinib 20 mg/kg, and 40 mg/kg groups were 1.8-, 2.0-, and 1.6-fold, respectively, higher than the corresponding mean ss C_b values ($p < 0.01$; Table 1, Fig. 1A). Comparison of TMZ steady-state concentrations in the tumor revealed that the mean ss C_t value in the sunitinib 20 mg/kg group was 17% and 46% higher than those in the control ($p > 0.05$) and sunitinib 60 mg/kg ($p < 0.05$) groups (Table 1, Fig. 1A), respectively. Because the plasma level of TMZ is an important factor driving the drug penetration into the tissue, the tissue-to-plasma steady-state concentration ratios for normal brain (ss C_b/C_p) and brain tumor (ss C_t/C_p) were calculated to correct for the variability of TMZ plasma levels in control and sunitinib-treated mice. Consistent with the ss C_b and ss C_t values, the mean ss C_b/C_p ratio was not different among the control and two sunitinib treatment groups, whereas the mean ss C_t/C_p ratio was significantly higher in the sunitinib 20 mg/kg groups compared with the control ($p < 0.05$) and sunitinib 60 mg/kg ($p < 0.01$) groups (Table 1, Fig. 1B). These data establish an important dose-dependent effect of sunitinib on TMZ brain tumor accumulation.

Effect of Sunitinib on Brain Tumor Vasculature

Our recent work has evaluated the effect of sunitinib on all three components of tumor vessels—endothelial cells,

Table 1. Steady-state pharmacokinetic parameters [mean ± SD (median, min–max)] of temozolomide (TMZ) in plasma, normal brain, and brain tumor in U87 glioma-bearing mice following a combined intravenous bolus dose (7.6 mg/kg) and a 3-h intraarterial infusion of TMZ (133.3 mg/kg/min) in control and sunitinib-treated mice

Parameters	Control	Sunitinib 20 mg/kg	Sunitinib 60 mg/kg
n	7	7	9
Tumor weight (mg)	111.5 ± 50.5	109.2 ± 38.0	78.4 ± 45.0
	(126.7, 27.6–170.0)	(118.7, 42.7–158.8)	(101.9, 8.6–140.7)
ss C_p (μg/ml)	18.6 ± 4.8	16.5 ± 2.9	16.6 ± 3.4
	(20.1, 11.2–23.3)	(16.3, 12.7–20.5)	(17.1, 12.2–21.1)
ss C_b (μg/ml)	7.6 ± 2.5	8.0 ± 1.7	7.1 ± 0.9
	(7.6, 3.0–11.0)	(8.4, 4.7–10.2)	(7.4, 5.7–7.9)
ss C_t (μg/ml)	13.9 ± 4.4*	16.3 ± 4.2*†	11.2 ± 2.4*
	(12.2, 9.6–21.2)	(16.0, 9.5–24.0)	(10.8, 8.0, 15.1)
ss C_b/C_p	0.408 ± 0.095	0.486 ± 0.080	0.441 ± 0.075
	(0.385, 0.268–0.545)	(0.500, 0.349–0.587)	(0.441, 0.351–0.570)
ss C_t/C_p	0.759 ± 0.172*	0.980 ± 0.167*‡§	0.681 ± 0.094*
	(0.841, 0.539–0.962)	(0.985, 0.711–1.206)	(0.669, 0.559–0.822)

Abbreviations: ss C_p, steady-state TMZ plasma concentration; ss C_b, steady-state TMZ normal brain concentration; ss C_t, steady-state TMZ tumor concentration. Statistical analysis are for one-way analysis of variance followed by the post hoc Tukey-Kramer multiple-comparison test.

*$p < 0.01$ compared with normal brain.

†$p < 0.05$ and ‡$p < 0.01$ compared with the sunitinib 60 mg/kg group.

§$p < 0.05$ compared with the control group.

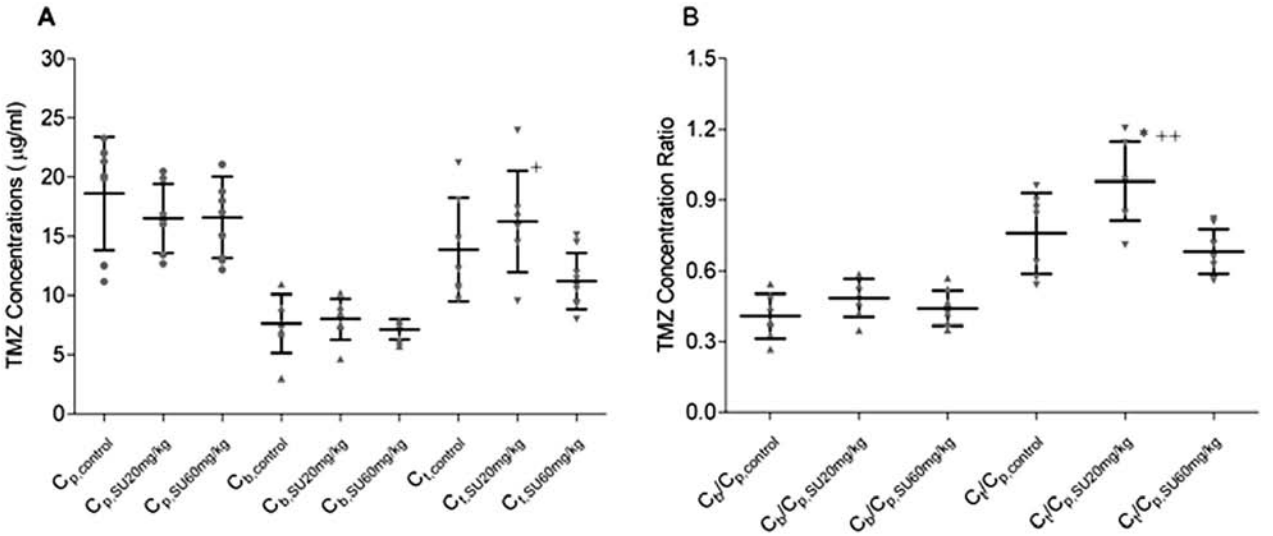

Fig. 1. (A) Steady-state temozolomide (TMZ) concentrations in the vehicle control (circles), sunitinib (SU) 20 mg/kg per day (triangles), and sunitinib 60 mg/kg per day treatment groups (inverted triangles). (B) Steady-state TMZ normal brain:plasma (triangles) and tumor:plasma (inverted triangles) concentration ratios. C_p, C_b, and C_t are the steady-state TMZ concentrations in plasma, normal brain, and brain tumor, respectively (mean ± SD). One-way analysis of variance followed by post hoc Tukey-Kramer multiple-comparison test: $^{*}p < 0.05$ compared with the control group; $^{+}p < 0.05$ and $^{++}p < 0.01$ compared with the sunitinib 60 mg/kg group.

mural cells, and blood vessel basement membranes—in a subcutaneous tumor model overexpressing VEGF.[30] To verify whether sunitinib exerted similar antiangiogenic activity in an intracerebral tumor, we examined the effect of sunitinib on the MVD, collagen VI, and α-SMA density in U87MG brain tumors using immunohistochemistry. The CD31-positive vessels in untreated U87MG brain tumors were abundant, tortuous, and variable in diameter (Fig. 2A). Similar to our findings in the subcutaneous tumor model, treatment with 20 mg/kg and 60 mg/kg of sunitinib for 7 days conspicuously reduced the tumor MVD by 56% and 76%, respectively ($p < 0.01$), and decreased the collagen IV density by 51% and 68%, respectively ($p < 0.01$), in a dose-dependent manner; however, no significant difference in the α-SMA density was observed between the control and two sunitinib treatment groups (Fig. 2B). Moreover, the mean VNI values, which were proposed in our recent study as the indication of the number of tumor vessels with relatively good quality,[30] were found to decrease in the order of 20 mg/kg sunitinib (0.9%) > vehicle control (0.6%) > 60 mg/kg sunitinib (0.5%). The difference in the VNI values was not significant among the three study groups (Fig. 2B).

Improved Brain Tumor Uptake of TMZ Due to the Vascular Normalization Effect of Sunitinib

To explore whether changes in the tumor vascularity were associated with the TMZ penetration into the brain tumor, we investigated whether the TMZ ss C_t/C_p ratios correlated with tumor MVD, collagen VI, and α-SMA density and with VNI. When the TMZ ss C_t/C_p ratios and immunostaining data from all animals were pooled, the TMZ ss C_t/C_p ratios significantly correlated with α-SMA density (Pearson correlation test, $p = 0.004$; Fig. 2C) and with VNI ($p = 0.014$; Fig. 2D). These results are consistent with the observations of our recent study demonstrating that α-SMA density and VNI significantly correlated with TMZ's tumor exposure, expressed as area under the unbound TMZ concentration–time curve, in tumor interstitial fluid in a subcutaneous tumor model.[24] Neither MVD nor collagen IV density significantly correlated with TMZ ss C_t/C_p ratios.

Assessment of Cell Proliferation and Apoptotic Cell Death in Tumor after Sunitinib Exposure

Immunohistochemical staining for Ki-67 protein, indicative of active cell proliferation, showed that the percentage of the Ki-67–positive cell population was 12% in the control group, while Ki-67 proliferation indices were significantly reduced by 48% and 56% in the sunitinib 20 mg/kg and 60 mg/kg groups, respectively ($p < 0.01$; Fig. 3A). Furthermore, the Ki-67 proliferation index was highly correlated with the MVD (Pearson correlation test, $p = 0.0003$; Fig. 3B) and the collagen IV density ($p = 0.000009$; Fig. 3C), whereas no significant correlation was found either between the Ki-67 proliferation index and the α-SMA density or between the Ki-67 proliferation index and the VNI. These results demonstrate that the observed antiproliferative effect of sunitinib in vivo was associated with its inhibitory effect on the tumor neovasculature. Because Ki-67 expression has been associated with a proliferative phenotype of malignant brain tumors,[35,36] this finding suggests that antiangiogenic therapy with sunitinib may be active against malignant brain tumors.

Few apoptotic cells were detected in the control and

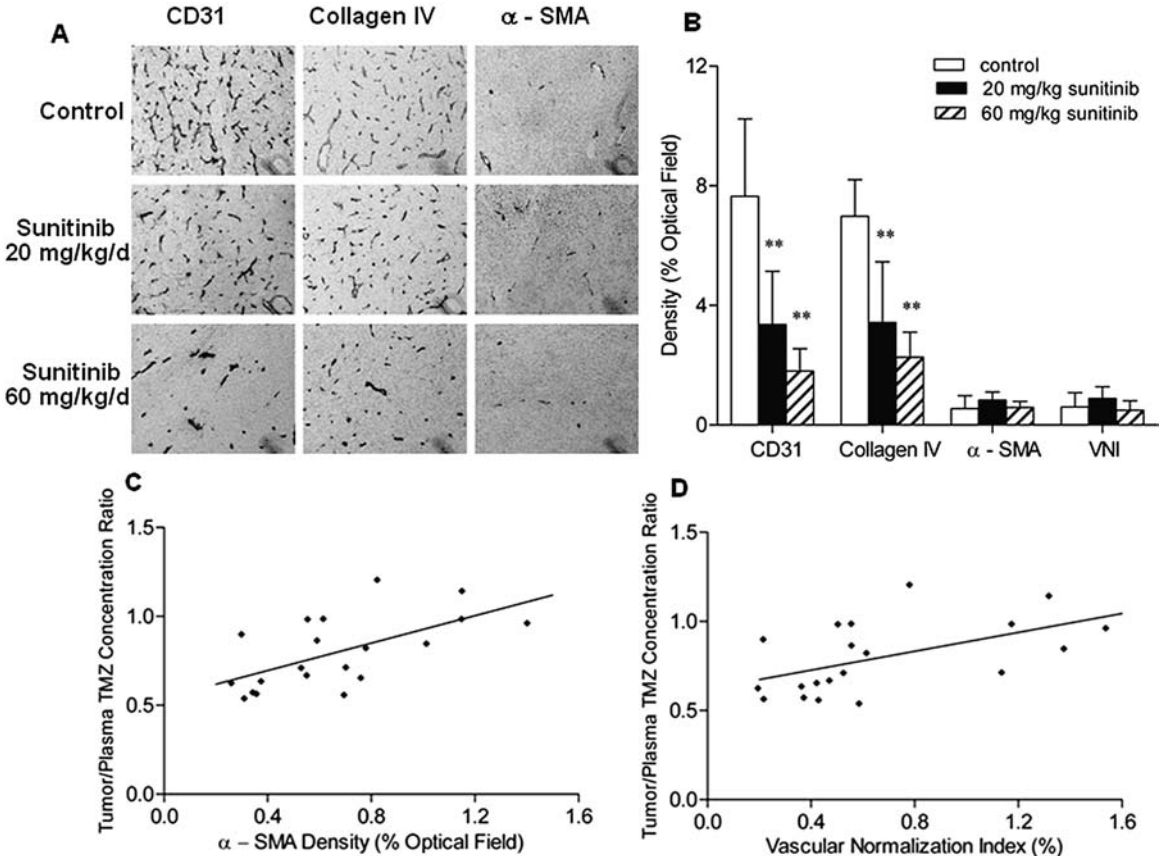

Fig. 2. The effect of sunitinib on the intratumoral vasculature within intracerebral U87MG xenografts and its impact on the brain tumor uptake of temozolomide (TMZ). (A) Representative examples for the detection of CD31, collagen IV, and α-smooth muscle actin (α-SMA) in tumor sections from the control and two sunitinib treatment groups. Original magnification, ×200. (B) Immunohistochemical analyses of microvessel density (MVD), collagen IV density, and α-SMA density in the U87MG tumor sections obtained from the control and 20 mg/kg and 60 mg/kg sunitinib-treated intracerebral tumor-bearing mice after the TMZ pharmacokinetic study as described in "Materials and Methods" (mean + SD). MVD and collagen IV density relative to the control tumors were significantly decreased in the sunitinib-treated tumors in a dose-dependent manner (**$p < 0.01$ compared with the control group, one-way analysis of variance followed by the post hoc Tukey-Kramer multiple-comparison test). (C) Steady-state TMZ tumor:plasma concentration ratio versus α-SMA density in the U87MG tumor sections ($r = 0.611$, $p = 0.004$, $n = 20$, Pearson's correlation test). (D) Steady-state TMZ tumor:plasma concentration ratio versus vascular normalization index value, calculated as MVD × ($\text{density}_{\alpha\text{-SMA}}/\text{density}_{\text{collagenVI}}$) ($r = 0.540$, $p = 0.014$, $n = 20$, Pearson's correlation test).

sunitinib-treated U87MG brain tumors. No significant difference in the apoptotic index was noted among the three study groups ($p > 0.05$; Fig. 3D).

Discussion

An increasing body of evidence shows that simultaneous targeting of the vascular and tumor compartments is an effective strategy in the treatment of cancer. In view of the serious practical limitations in obtaining tumor samples in clinical studies, the potential of new combination therapies for brain tumors can be explored in appropriate experimental models to obtain essential information in support of their clinical use. Given that the typical recommended dose for TMZ is 200 mg/m^2 orally daily for 5 consecutive days every 4 weeks[37] and for sunitinib is 50 mg orally once daily for 4 weeks on/2 weeks off,[17] it is likely that TMZ would be given concurrently with sunitinib in a clinical setting, so analysis of the combination in a preclinical brain tumor model could reveal important interactions.

In this study, we investigated the effect of sunitinib at two different dose levels on the brain tumor accumulation of TMZ in an orthotopic brain tumor model, which should more closely resemble brain tumors in patients compared with subcutaneous tumor models. An important determinant of drug distribution in brain is the restrictive BBB, which, although compromised due to the presence of a tumor, is still a restrictive variable for drug penetration that cannot be duplicated in a subcutaneous model. Although the reported oral maximum tolerated dose of sunitinib for the treatment of gliomas in the preclinical studies was 80 mg/kg per day,[12,16] significant body weight loss and severe diarrhea were observed in animals treated with sunitinib at a daily oral dose of 80 mg/kg in our pilot study (data not shown). Therefore, for the high-dose sunitinib treatment group, mice

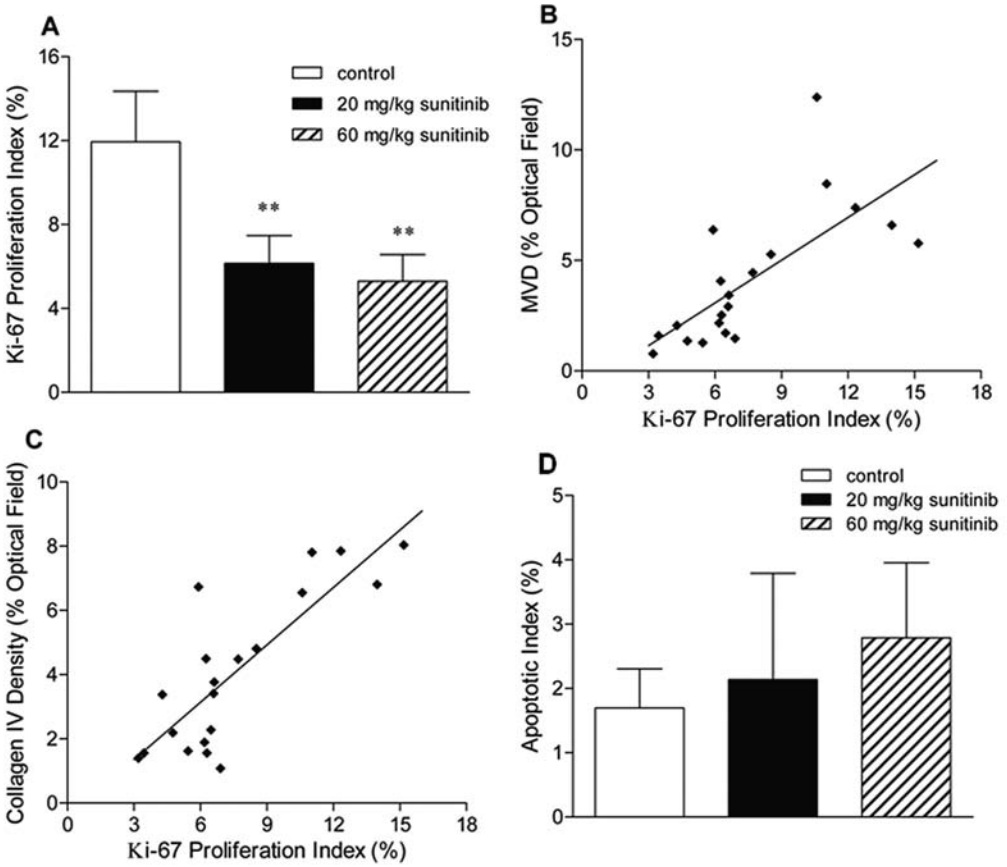

Fig. 3. Antitumor activity of sunitinib in mice bearing intracerebral U87MG human gliomas. Nude mice bearing established intracerebral U87MG gliomas (24 days after tumor implantation) were randomized into three groups receiving daily oral administration of vehicle, 20 mg/kg sunitinib, or 60 mg/kg sunitinib for 7 days. (A) The effect of sunitinib on cell proliferation assessed by Ki-67 immunostaining (mean + SD). Ki-67 proliferation index = (number of Ki-67-positive cells/total number of cells) × 100%. One-way analysis of variance followed by post hoc Tukey-Kramer multiple-comparison test: $^{**}p < 0.01$ compared with the control group. (B) Microvessel density versus Ki-67 proliferation index in the U87MG tumor sections ($r = 0.720$; $p = 0.0003$, $n = 20$, Pearson's correlation test). (C) Collagen IV density versus Ki-67 proliferation index in the U87MG tumor sections ($r = 0.822$; $p = 0.000009$, $n = 20$, Pearson's correlation test). (D) The effect of sunitinib on apoptosis assessed by terminal deoxynucleotidyl transferase-mediated 2'-deoxyuridine 5'-triphosphate nick-end labeling (TUNEL) assay.

were given 60 mg/kg of sunitinib daily for 7 days, which corresponded to a cumulative dose of 420 mg/kg and was comparable to the total of the five daily treatments of 80 mg/kg sunitinib based on the reported effective regimen of a 5-day-on/2-day-off schedule.[16] For the low-dose sunitinib treatment, a daily oral dose of 20 mg/kg sunitinib was chosen to provide a 3-fold dose range yet still provide a dose level reported to be effective in most solid tumor models.[12]

In the present study we did not attempt to determine unbound TMZ concentration in the tumor extracellular fluid using microdialysis, as we did in the subcutaneous tumor model study, because obtaining microdialysis samples from brain tumors of mice was found to be difficult due to the size constraints of the probe diameter relative to the size of the tumor—it was difficult to ensure samples were collected from within the tumor and not adjacent tumor tissue. Our previous study in rats demonstrated that TMZ concentrations obtained from tumor homogenates were consistent with those from microdialysis.[38] Therefore, the PK approach used in this study, which was based on steady-state TMZ concentrations in plasma and brain, derived from tissue homogenates, avoided technical issues related to microdialysis sampling and provided an accurate indication of TMZ's brain distribution.

TMZ is thought not to undergo any specialized membrane transport processes, but to enter and exit cells via passive diffusion. Passive transport of compounds across the BBB is dependent on the lipophilicity, molecular weight, and degree of ionization at physiological pH[39,40] and can be limited by either cerebral blood flow (i.e., perfusion limited) or permeability (i.e., diffusion limited). Theoretically, perfusion-limited BBB transport is applicable for lipophilic, small, and noncharged drugs, such as chloroethylnitrosoureas and procarbazine, whereby diffusion is via transcellular route and not rate limiting, whereas BBB penetration of the more hydrophilic drugs depends on capillary permeability. Based on the equation proposed by Levin[41]—log permeability (cm/s) = –4.605 + 0.4115 log (P/MW$^{1/2}$), where P is the octanol/water partition coefficient and MW is molecular weight—the

brain capillary permeability value for TMZ would be 2.7×10^{-6} cm/s using a reported octanol/water partition coefficient or log *D* value of –1.03 for TMZ at physiological pH.[42] A brain capillary permeability value of 1×10^{-6} cm/s was considered low permeability, whereas 1×10^{-4} cm/s was considered high, thus placing TMZ in the low-permeability category. Extending this analysis to drug transport in a brain tumor model, we can consider an early study of transcapillary exchange of various drugs and standard molecules in the intracerebral 9L rat tumor model.[41] That study demonstrated that, for compounds with good penetration of the BBB, as indicated by the high brain capillary transfer constant (K_i) values, the K_i values in tumor were lower than those in normal brain, because the delivery of those compounds was controlled more by the blood flow (i.e., perfusion-limited), which was found to be lower in the 9L tumor than in the normal rat brain.[41] In the present study, the steady-state TMZ concentrations in tumor were significantly higher than those in the normal brain, most likely due to a compromised tumor vasculature, suggesting that the distribution of TMZ tends to be more diffusion limited. The findings of the present study therefore support the notion that, for compounds with generally lower BBB permeability values, penetration in the tumor is higher than that in the normal brain.[41]

The results of the TMZ PK study demonstrate that sunitinib given at a dose level of 20 mg/kg significantly increased TMZ levels in the brain tumor without affecting the systemic exposure to TMZ and the penetration of TMZ to normal brain. In contrast, sunitinib treatment at the higher 60 mg/kg dose tended to decrease brain tumor accumulation of TMZ (Table 1, Fig. 1). Further examination of the angiogenic biomarkers in tumor sections using immunostaining revealed that sunitinib treatment significantly reduced brain tumor MVD and collagen IV density in a dose-dependent manner but had no effect on the α-SMA density, demonstrating that sunitinib treatment mainly targets tumor-associated endothelial cells but has little effect on the mural cells. Using these end points, we proposed a composite VNI in our recent study to indicate the fraction of functioning vessels out of the total number of tumor vessels.[30] In the present study, VNI values were greatest in the 20 mg/kg sunitinib treatment group, followed by the control group and 60 mg/kg sunitinib treatment group, indicating more functioning vessels in the 20 mg/kg sunitinib-treated tumors compared with those in the control and 60 mg/kg sunitinib-treated tumors. The lower fraction of function vessels in the high-dose 60 mg/kg sunitinib group was associated with extensive vascular regression, as indicated by the low MVD, and may have been instrumental in abating TMZ penetration because less capillary surface area is available for drug transport. Further studies will be helpful to delineate the drug transport mechanisms underpinning the positive relationships between TMZ tumor distribution and the VNI. Such positive correlations, also found in our prior study,[30] highlight the potential of using VNI as a quantitative criterion to select antiangiogenic therapy with coadministered cytotoxic drugs that has the most positive effect in terms of tumor uptake. Further employment of VNI-based dosing strategies could also be seen as a means to reduce dose levels of cytotoxic agents, such as TMZ, to minimize systemic toxicities while still achieving toxic concentrations in brain tumors.

It is noteworthy that Claes et al.[43] recently reported that vandetanib, a selective inhibitor of VEGFR and epidermal growth factor receptor tyrosine kinases, interfered with the therapeutic activity of TMZ in a murine intracerebral U87 tumor model. The deleterious effects of vandetanib on TMZ's activity were based on a reduction in TMZ-induced apoptosis in intracerebral tumors that was attributed to restoration of the BBB, partially supported by MRI data, and obstruction of TMZ's intratumoral distribution. Although we cannot directly compare our results and those of Claes et al. because different drugs (vandetanib vs. sunitinib), dosing schedules (more prolonged antiangiogenic therapy in the Claes et al. study), and end points (TMZ concentrations were not measured in the Claes et al. study) were evaluated, results of these studies may represent part of the same spectrum of effects caused by antiangiogenic therapy. Although the Claes et al. group believes that vessel normalization in brain has an antagonistic effect on TMZ,[43] they indicate, with data supported by another study,[44] that lower doses of vandetanib inhibited angiogenesis while not affecting a disrupted BBB. This dose-dependent action of an angiogenesis inhibitor would coincide with our results, which are based on TMZ concentration measurements, and supports the possibility that a certain vascular normalization window has to be achieved for successful combination regimens of cytotoxic drugs and angiogenesis inhibitors.[28]

Slices of tumor samples obtained from the sunitinib-treated animals showed a significant reduction in the number of proliferating cells and a mild increase in cells undergoing programmed cell death. Moreover, the fraction of Ki-67–positive cells in the tumor section was found to be highly correlated to the tumor MVD and collagen IV density (Fig. 3B,C). These observations were analogous to those from previous studies using sunitinib alone or in combination with conventional modalities, for example, radiotherapy and cytotoxic chemotherapy.[45,46] Guérin et al.[45] studied combined therapy with sunitinib, cetuximab, and docetaxel in a prostate tumor model and demonstrated a parallel diminution in both tumor cell proliferation and vascularization when sunitinib was used alone or in combination. Moreover, sunitinib alone had no significant effect on the induction of apoptosis but had to be combined with docetaxel to achieve greater induction of apoptosis. A study by Schueneman et al.,[46] using sunitinib with fractionated radiotherapy in murine Lewis lung carcinoma and GL261 glioblastoma multiform models, showed that sunitinib followed by irradiation resulted in positive TUNEL staining only in endothelial cells, indicating that the predominant effect of sunitinib may be at the level of tumor vascular endothelium. No published data address the time it may take to induce apoptosis by TMZ; however, given the mechanism of cell death, attributed to the formation of O^6-methylguanine DNA

adducts, and mismatch pairing with thymine during subsequent cycles of DNA replication, followed by persistent daughter-strand breakage,[47] it is unlikely that the observed apoptosis in the tumor at the end of the 3-h TMZ infusion could be solely attributed to TMZ. Thus, it seems likely that the mild increase in the fraction of TUNEL-positive cells in the sunitinib treatment groups could be mainly attributed to the increased number of apoptotic endothelial cells in tumors.

In conclusion, the results obtained from this study demonstrate that antiangiogenic therapy with sunitinib at an appropriate dose can positively alter the tumor vasculature to improve the penetration of TMZ into brain tumors. Moreover, our data support continued analysis of dose- and time-dependent effects of angiogenesis inhibitors on the tumor vasculature and the VNI as a means to correlate the angiogenic phenotype to the distribution of cytotoxic drugs into tumors. Finally, our findings could affect strategies for combination chemotherapy in malignant glioma patients.

Acknowledgment

This work was supported by National Institutes of Health grant CA72937.

References

1. DeAngelis LM. Brain tumors. *N Engl J Med*. 2001;344:114–123.
2. Senger D, Cairncross JG, Forsyth PA. Long-term survivors of glioblastoma: statistical aberration or important unrecognized molecular subtype? *Cancer J*. 2003;9:214–221.
3. Reardon DA, Rich JN, Friedman HS, Bigner DD. Recent advances in the treatment of malignant astrocytoma. *J Clin Oncol*. 2006;24:1253–1265.
4. Leon SP, Folkerth RD, Black PM. Microvessel density is a prognostic indicator for patients with astroglial brain tumors. *Cancer*. 1996;77:362–372.
5. Wesseling P, van der Laak JA, Link M, Teepen HL, Ruiter DJ. Quantitative analysis of microvascular changes in diffuse astrocytic neoplasms with increasing grade of malignancy. *Hum Pathol*. 1998;29:352–358.
6. Folkman J, Watson K, Ingber D, Hanahan D. Induction of angiogenesis during the transition from hyperplasia to neoplasia. *Nature*. 1989;339:58–61.
7. Hanahan D, Folkman J. Patterns and emerging mechanisms of the angiogenic switch during tumorigenesis. *Cell*. 1996;86:353–364.
8. Kesisis G, Broxterman H, Giaccone G. Angiogenesis inhibitors. Drug selectivity and target specificity. *Curr Pharm Des*. 2007;13:2795–2809.
9. Jouanneau E. Angiogenesis and gliomas: current issues and development of surrogate markers. *Neurosurgery*. 2008;62:31–50.
10. Albini A, Noonan DM, Ferrari N. Molecular pathways for cancer angioprevention. *Clin Cancer Res*. 2007;13:4320–4325.
11. Sun L, Liang C, Shirazian S, et al. Discovery of 5-[5-fluoro-2-oxo-1,2-dihydroindol-(3Z)-ylidenemethyl]-2,4-dimethyl-1H-pyrrole-3-carboxylic acid (2-diethylaminoethyl)amide, a novel tyrosine kinase inhibitor targeting vascular endothelial and platelet-derived growth factor receptor tyrosine kinase. *J Med Chem*. 2003;46:1116–1119.
12. Mendel DB, Laird AD, Xin X, et al. In vivo antitumor activity of SU11248, a novel tyrosine kinase inhibitor targeting vascular endothelial growth factor and platelet-derived growth factor receptors: determination of a pharmacokinetic/pharmacodynamic relationship. *Clin Cancer Res*. 2003;9:327–337.
13. Abrams TJ, Lee LB, Murray LJ, Pryer NK, Cherrington JM. SU11248 inhibits KIT and platelet-derived growth factor receptor beta in preclinical models of human small cell lung cancer. *Mol Cancer Ther*. 2003;2:471–478.
14. O'Farrell AM, Abrams TJ, Yuen HA, et al. SU11248 is a novel FLT3 tyrosine kinase inhibitor with potent activity in vitro and in vivo. *Blood*. 2003;101:3597–3605.
15. Chow LQ, Eckhardt SG. Sunitinib: from rational design to clinical efficacy. *J Clin Oncol*. 2007;13:1367–1373.
16. de Boüard S, Herlin P, Christensen JG, et al. Antiangiogenic and anti-invasive effects of sunitinib on experimental human glioblastoma. *Neuro-Oncology*. 2007;9:412–423.
17. Goodman VL, Rock EP, Dagher R, et al. Approval summary: sunitinib for the treatment of imatinib refractory or intolerant gastrointestinal stromal tumors and advanced renal cell carcinoma. *Clin Cancer Res*. 2007;13:1367–1373.
18. Medioni J, Cojocarasu O, Belcaceres JL, Halimi P, Oudard S. Complete cerebral response with sunitinib for metastatic renal cell carcinoma. *Ann Oncol*. 2007;18:1282–1283.
19. Koutras AK, Krikelis D, Alexandrou N, Starakis I, Kalofonos HP. Brain metastasis in renal cell cancer responding to sunitinib. *Anticancer Res*. 2007;27:4255–4257.
20. Helgason HH, Mallo HA, Droogendijk H, et al. Brain metastases in patients with renal cell cancer receiving new targeted treatment. *J Clin Oncol*. 2008;26:152–154.
21. Leenders WP, Küsters B, de Waal RM. Vessel co-option: how tumors obtain blood supply in the absence of sprouting angiogenesis. *Endothelium*. 2002;9:83–87.
22. Holash J, Maisonpierre PC, Compton D, et al. Vessel cooption, regression, and growth in tumors mediated by angiopoietins and VEGF. *Science*. 1999;284:1994–1998.
23. Pezzella F, Pastorino U, Tagliabue E, et al. Non-small-cell lung carcinoma tumor growth without morphological evidence of neo-angiogenesis. *Am J Pathol*. 1997;151:1417–1423.
24. Vermeulen PB, Colpaert C, Salgado R, et al. Liver metastases from colorectal adenocarcinomas grow in three patterns with different angiogenesis and desmoplasia. *J Pathol*. 2001;195:336–342.
25. Rubenstein JL, Kim J, Ozawa T, et al. Anti-VEGF antibody treatment of glioblastoma prolongs survival but results in increased vascular cooption. *Neoplasia*. 2000;2:306–314.
26. Kunkel P, Ulbricht U, Bohlen P, et al. Inhibition of glioma angiogenesis and growth in vivo by systemic treatment with a monoclonal antibody against vascular endothelial growth factor receptor-2. *Cancer Res*. 2001;61:6624–6628.

27. van Kempen LC, Leenders WP. Tumours can adapt to anti-angiogenic therapy depending on the stromal context: lessons from endothelial cell biology. *Eur J Cell Biol*. 2006;85:61–68.
28. Jain RK. Normalization of tumor vasculature: an emerging concept in antiangiogenic therapy. *Science*. 2005;307:58–62.
29. Dickson PV, Hamner JB, Sims TL, et al. Bevacizumab-induced transient remodeling of the vasculature in neuroblastoma xenografts results in improved delivery and efficacy of systemically administered chemotherapy. *Clin Cancer Res*. 2007;13:3942–3950.
30. Zhou Q, Guo P, Gallo JM. Impact of angiogenesis inhibition by sunitinib on tumor distribution of temozolomide. *Clin Cancer Res*. 2008;14:1540–1549.
31. Taghian AG, Suit HD. Animal systems for translational research in radiation oncology. *Acta Oncol*. 1999;38:829–838.
32. Claes A, Schuuring J, Boots-Sprenger S, et al. Phenotypic and genotypic characterization of orthotopic human glioma models and its relevance for the study of anti-glioma therapy. *Brain Path*. 2008;18:423–433.
33. Ma J, Li S, Reed K, Guo P, Gallo JM. Pharmacodynamic-mediated effects of the angiogenesis inhibitor SU5416 on the tumor disposition of temozolomide in subcutaneous and intracerebral glioma xenograft models. *J Pharmacol Exp Ther*. 2003;305:833–839.
34. Stewart DJ. A critique of the role of the blood-brain barrier in the chemotherapy of human brain tumors. *J Neurooncol*. 1994;20:121–139.
35. Johannessen AL, Torp SH. The clinical value of Ki-67/MIB-1 labeling index in human astrocytomas. *Pathol Oncol Res*. 2006;12:143–147.
36. Donato V, Papaleo A, Castrichino A, et al. Prognostic implication of clinical and pathologic features in patients with glioblastoma multiforme treated with concomitant radiation plus temozolomide. *Tumori*. 2007;93:248–256.
37. Payne MJ, Pratap SE, Middleton MR. Temozolomide in the treatment of solid tumours: current results and rationale for dosing/scheduling. *Crit Rev Oncol Hematol*. 2005;53:241–252.
38. Ma J, Pulfer S, Li S, Chu J, Reed K, Gallo JM. Pharmacodynamic-mediated reduction of temozolomide tumor concentrations by the angiogenesis inhibitor TNP-470. *Cancer Res*. 2001;61:5491–5498.
39. Oldendorf WH. Blood-brain barrier permeability to drugs. *Annu Rev Pharmacol*. 1974;14:239–248.
40. Levin VA. Relationship of octanol/water partition coefficient and molecular weight to rat brain capillary permeability. *J Med Chem*. 1980;23:682–684.
41. Levin VA. Pharmacokinetics and central nervous system chemotherapy. In: Hellmann K, Carter SK, eds. *Fundamentals of Cancer Chemotherapy*. New York: McGraw-Hill; 1987:28–40.
42. Thomas F, Rudraraju V, Lockman P, Smith Q. Blood-brain barrier permeability and transport of temozolomide [abstract]. *AAPS PharmSci*. 2007;1646. Available at http://www.aapsj.org/abstracts/AM_2007/AAPS2007-001646.PDF. Accessed February 5, 2008.
43. Claes A, Wesseling P, Jeuken J, Maass C, Heerschap A, Leenders WP. Antiangiogenic compounds interfere with chemotherapy of brain tumors due to vessel normalization. *Mol Cancer Ther*. 2008;7:71–78.
44. Leenders WP, Küsters B, Verrijp K, et al. Antiangiogenic therapy of cerebral melanoma metastases results in sustained tumor progression via vessel co-option. *Clin Cancer Res*. 2004;10:6222–6230.
45. Guérin O, Formento P, Lo Nigro C, et al. Supra-additive antitumor effect of sunitinib malate (SU11248, Sutent) combined with docetaxel. A new therapeutic perspective in hormone refractory prostate cancer. *J Cancer Res Clin Oncol*. 2008;134:51–57.
46. Schueneman AJ, Himmelfarb E, Geng L, et al. SU11248 maintenance therapy prevents tumor regrowth after fractionated irradiation of murine tumor models. *Cancer Res*. 2003;63:4009–4016.
47. Friedman HS, Kerby T, Calvert H. Temozolomide and treatment of malignant glioma. *Clin Cancer Res*. 2000;6:2585–2597.